International Journal of Fluid Machinery and Systems
Vol. 8, No. 3, July-September 2015

DOI: 10.5293/IJFMS.2015.8.3.209
ISSN (Online): 1882-9554

Original Paper

Physics-based Surrogate Optimization of Francis Turbine Runner Blades, Using Mesh Adaptive Direct Search and Evolutionary Algorithms

Salman Bahrami[1], Christophe Tribes[1], Sven von Fellenberg[2], Thi C. Vu[2] and François Guibault[3]

[1]Department of Mechanical Engineering, École Polytechnique de Montréal
Montreal, QC, H3T 1J4, Canada, salman.bahrami@polymtl.ca, christophe.tribes@polymtl.ca
[2]R&D Division, Andritz Hydro Canada Inc.
6100, aut. Transcanadienne, Point-Claire, QC, H9R 1B9, Canada, sven.vonfellenberg@andritz.com, thi.vu@andritz.com
[3]Department of Computer Engineering, École Polytechnique de Montréal
Montreal, QC, H3T 1J4, Canada, francois.guibault@polymtl.ca

Abstract

A robust multi-fidelity optimization methodology has been developed, focusing on efficiently handling industrial runner design of hydraulic Francis turbines. The computational task is split between low- and high-fidelity phases in order to properly balance the CFD cost and required accuracy in different design stages. In the low-fidelity phase, a physics-based surrogate optimization loop manages a large number of iterative optimization evaluations. Two derivative-free optimization methods use an inviscid flow solver as a physics-based surrogate to obtain the main characteristics of a good design in a relatively fast iterative process. The case study of a runner design for a low-head Francis turbine indicates advantages of integrating two derivative-free optimization algorithms with different local- and global search capabilities.

Keywords: Physics-based surrogate optimization, Francis turbine runner blade, multi-fidelity algorithm

1. Hydraulic Turbine Design Optimization Process

Big changes in global energy demand, increasing environmental concerns, and growth potential of cost-efficient hydroelectric energy, have recently resulted in more demand to design hydraulic turbines which are more efficient and durable. As design challenges are getting more complex, runner designers rely more than ever on engineering and simulation tools, especially computational fluid dynamics (CFD), to obtain reliable designs with a competitive time and cost. Although runner designers already employ CFD tools to evaluate their designs, there is a strong need to integrate CFD analyses more tightly in the design chain using efficient optimization methods to obtain more efficient design processes.

The full range of CFD methods have been utilized in the optimization of hydraulic turbine runner blades. Low-fidelity inviscid models (e.g. potential flow) have been employed by some researches such as Holmes and McNabb [1]. However, they are not accurate enough in their prediction of flow behavior, mainly due to lack of physics. High-fidelity viscous models have been used alone to optimize the runner as well (e.g. using turbulent RANS solvers, by Franco-Nava et al. [2] and Pilev et al. [3]); but they are too expensive and slow for iterative industrial runner design processes. To reduce high-fidelity analyses in the optimization loop, surrogate-based optimization approaches have been increasingly employed by researchers, using either mathematical surrogates or physic-based surrogates. Mathematical surrogates are computationally inexpensive approximation models constructed from a given number of high-fidelity evaluations. For instance, artificial neural network was applied by Derakhshan et al. [4] to reduce Navier-Stokes solver calls during the optimization of a low-head axial hydro turbine by an evolutionary algorithm. Another popular mathematical surrogate, radial basis functions, was employed by Georgopoulou et al. [5].

Although those mathematical surrogates have been used for blade shape optimizations, they still require a large number of high-

Received January 15 2015; revised March 20 2015; accepted for publication September 9 2015: Review conducted by Prof. Soon-Wook Kim. (Paper number O15047S)
Corresponding author: Salman Bahrami, salman.bahrami@polymtl.ca

This paper was presented at the 27th IAHR Symposium on Hydraulic Machinery and Systems, September 4, Montreal, Canada.

fidelity viscous evaluations to update and to ensure that they yield reasonably accurate results. For this reason, physics-based surrogate can be a better alternative in some situations, which uses simplified physics of the problem (i.e. low-fidelity evaluations). Physics-based surrogates are usually used in multi-fidelity frameworks mainly in order to correct low-fidelity evaluations of objectives and constraints using high-fidelity results.

Beside all the aforementioned researches, industrial runner design process currently relies extensively on the designer's intuition and experience, using both inviscid and viscous flow analyses, but mostly without using an optimizer. Runner designers can use fast inviscid flow solvers, to carry out most design iterations in early phase of the design process. The high-fidelity analyses are also considered to further assess the design quality. To fulfil industrial design needs, a new practical multi-fidelity methodology has been developed using a physics-based surrogate optimization in the low-fidelity phase. In this methodology the optimizer employs a computationally-cheap inviscid flow solver in the low-fidelity phase. The low-fidelity optimization problem is corrected by accurate high-fidelity information in an overall design loop. Previous investigations (e.g. by Alexandrov et al. [6], Robinson et al. [7], and by Leifsson and Koziel [8]) indicate that multi-fidelity methods require much fewer high-fidelity evaluations than mathematical surrogates to obtain a given level of accuracy. To comply with runner designers' approaches, the proposed design framework involves all existing design resources (see Fig. 1), adding an automatic optimization loop to decrease designer interactions.

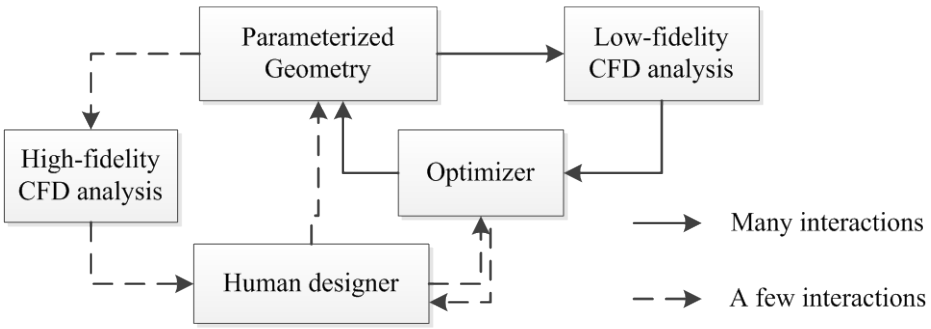

Fig. 1 Runner design loop interactions

In the next section, the multi-fidelity optimization methodology is presented. In section 3, a case study is presented using a low-head Francis runner. Even though we presented the multi-fidelity methodology using the same test case in 27th IAHR Symposium on Hydraulic Machinery and Systems [9], the current enhanced paper focuses on how the exploration capabilities of optimization methods affect the optimization efficiency and robustness to obtain good Francis runner designs. Mesh adaptive direct search (MADS) and evolutionary algorithm have been employed, which are mostly well-known as good local- and global search methods respectively. Among different types of derivative-free optimization methods, these two methods have demonstrated their abilities in hydraulic optimization problems.

2. Multi-Fidelity Design Optimization Methodology

2.1 Low-Fidelity Phase

The main iterative computations are carried out in the low-fidelity phase which contains the low-fidelity optimization loop (see Fig. 2). It aims to approach the main design characteristics via thousands of fast and computationally inexpensive low-fidelity (i.e. inviscid flow) evaluations within an optimization loop. This loop starts with a parameterized model using a few design variables representing the initial geometry. Inviscid flow field calculations produce the required information, such as velocity and pressure distributions on the blade, to evaluate objective functions and constraints. The optimizer determines new design variable values, based on the improvement or deterioration in the objective and constraint values. Since inviscid flow solvers cannot consider viscous effects, the low-fidelity optimization phase focuses on meeting specific target flow characteristics that are indirectly associated with low energy losses (equivalently high machine efficiency) and cavitation absence at the given operating conditions. In this project, a potential flow solver has been chosen as the physics-based surrogate.

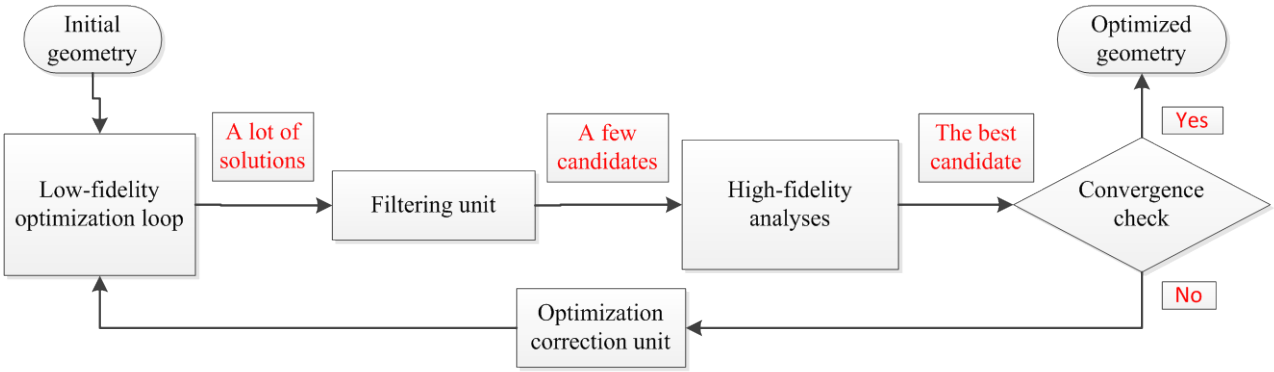

Fig. 2 Multi-fidelity design optimization algorithm

In this investigation, the low-fidelity evaluations cannot be used to determine derivative information with enough accuracy. Moreover, the complexity of the design space and presence of many local optimums requires both local and global design space explorations. For these reasons, we have selected two different derivative-free optimization methods. NOMAD (Non-smooth Optimization by Mesh Adaptive Direct Search) [10] has been selected as an open source [11] C++ implementation of the Mesh Adaptive Direct Search algorithm [12]. Also, a well-known evolutionary algorithm has been used by employing an optimization code, evolutionary algorithm system (EASY) [13]. It has been used in similar investigations, such as Francis runner and radial pump impeller optimization [14] and draft tube optimization [15]. The details of this optimizer and evolutionary algorithm can be found in [16].

2.2 Filtering Process

Based on the number of objectives, the dominant solution or a set of them (i.e. Pareto optimal solutions) can be identified after the low-fidelity optimization. However, differences between low-fidelity optimization results and high-fidelity Navier-Stokes results are expected, which are due to assumptions made through the use of inviscid flow evaluations. Preliminary investigations have shown that other feasible optimization solutions, not too far from dominant solutions, can also bring high efficiency in Navier-Stokes evaluations. Therefore, a versatile filtering algorithm (filtering unit in Fig. 2) has been developed to select a few promising candidates which are geometrically different and dominant in their own territories. These candidates are transferred to the high-fidelity phase for Navier-Stokes evaluations.

The filtering process contains the following parts:

- Filtering feasible optimization solutions.
- Mapping the design space into a distributing standard hypercube.
- Distributing those solutions into small unit-length hypercubes.
- Selecting one dominant candidate from each unit-length hypercube.
- Selecting a few geometrically-different candidates out of all selected candidates via a clustering method.

The details of proposed filtering process are available in [17].

2.3 High-Fidelity Phase

In the high-fidelity phase, a viscous flow solver is used to accurately evaluate a few selected candidates. It aims to choose the best design candidate which has a good efficiency at the right operating condition, and minimum cavitation. This design candidate may be transferred into the low-fidelity phase as a new initial design for the next optimization step, or selected as the final design based on certain convergence criteria or computational budget limit. The number of design variables of the best candidate may be increased when it is transferred, mainly in order to give more flexibility to the optimizer to satisfy real constraints in the next step. By analyzing the results of the high-fidelity phase, it is possible to recalibrate the objectives and constraints, in order to obtain the desired results and expected final goals in the high-fidelity phase.

The commercial Navier-Stokes code ANSYS-CFX has been employed for the flow field simulations using the standard two-equation k-ε RANS turbulence model. Due to rotational periodic conditions, the viscous flow analysis is performed only for a single passage of the runner flow. This domain is discretized using approximately 200,000 structured cells. Details of the methodology, integrated tools and validations can be found in the references [18-20].

3. Low-Fidelity Optimization Arrangement

All multi-fidelity optimization formulations including the low-fidelity optimization problem have been presented extensively in [21]. The low-fidelity optimization problem is formulated as:

Minimizing $f_i(y)$

Subject to $g_j(y) \le 0 \quad ; \quad y_l \le y \le y_u$

Where "y" is the N-dimensional vector of design variables, and "y_l" and "y_u" are respectively the lower and upper bounds of design variables. One objective and three constraints have been defined in this project.

3.1 Objective and Constraints

Previous investigations have shown that minimizing the length of the blade is a good way to drive the optimization towards good runner geometries. The objective function is calculated from summation of weighted section lengths.

Different types of constraints may be used in hydraulic runner optimization. For this investigation, three constraints control the most important design criteria addressing minimum losses and maximum efficiency at the targeted operating condition:

- Velocity constraint: To control the losses in the draft tube, it is necessary that the runner delivers an appropriate tangential velocity profile at the draft-tube inlet [22, 23]. Therefore, this velocity component at the runner outlet reference line has been determined to be similar to a targeted profile within a safe bound, which is based on designers' experiences.
- Blade loading: one constraint prevents negative blade loading on all blade sections.
- Cavitation: one constraint has been defined to limit the minimum allowed pressure for all blade sections, in order to represent cavitation issues during the optimization.

3.2 Initial Geometry and Design Variables

A low-head Francis turbine runner has been chosen. The goal is to design a runner such that on a given efficiency curve (speed coefficient N_{ed} equal to 0.407) it provides the peak position at a given flow coefficient P_{ed} equal to 0.294. This turbine contains 13 runner blades and 20 guide vanes. The initial geometry is a poor hydraulic blade shape.

Figure 3(a) shows blade edges and runner inner/outer contours, projected in the meridional plane. The tangential velocity reference line has been shown as well. Figure 3(b) illustrates the simple geometry of the initial blade. Figure 3(c) shows the aggregated fluid flow domain considered in the computational analyses. Inlet and outlet boundaries are illustrated on the top and bottom of the blade respectively. Figure 3(d) illustrates the whole runner considering rotational periodicity of the flow domain. The blade thickness has been created using a NACA blade thickness profile (see Fig. 4).

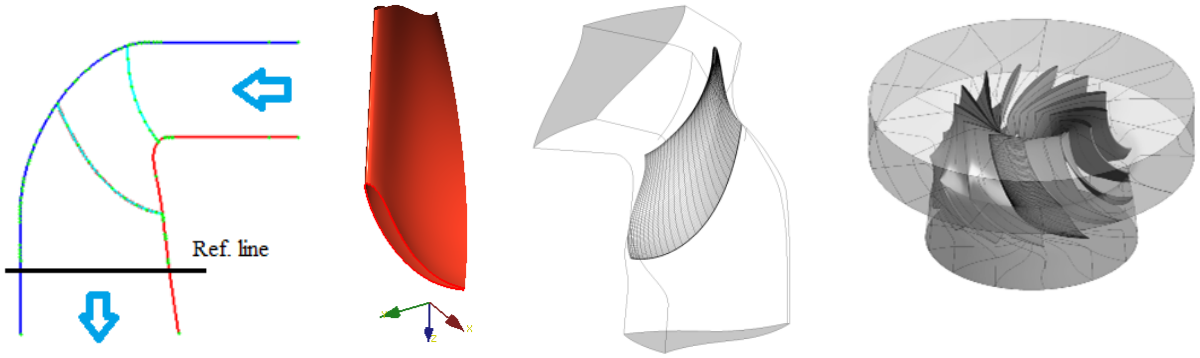

(a) (b) (c) (d)

Fig. 3 Initial blade geometry, single-blade and runner flow computational domain

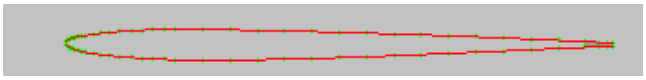

Fig. 4 Blade thickness profile

Blade geometries are parameterized through an in-house software developed by Andritz Hydro Canada Inc. [24]. The software allows changing the number of parameters representing the geometry, modifying each of them, and visualizing the geometrical model.

Table 1 shows the main geometric parameters and design variables. Curvature of the blade is governed by some angle control points along streamline sections from the leading edge to the trailing edge. The lean of the leading edge is represented by other angle points on a 2D projected curve from band to crown. Blade length is defined by the camber line length in each section. The band-side contour is optimized using cylindrical coordinates (i.e. r and z) of two points located downstream of the leading edge on the band. Proper bounds of variations are defined for each four types of design variables, based on some geometric limits and/or designer experiences.

Table 1 Number of independent parameters & design variables

	Initial model parameters	*Optimization design variables*
Blade curvature	9	9
Blade length	11	3
Blade leading edge	11	1
Band contour	20	4
Crown contour	43	Fixed
Blade thickness	80	Fixed
Number of blades	13	Fixed

3.3 Optimization Features

A maximum number of 40,000 low-fidelity evaluations have been set for both optimizers. Also, the same problem formulations has been used for both optimizers.

Although only one objective is used for the problem at hand, it should be noted that both optimizers are able to handle multi-objective optimization problems. For instance, we presented the results of a bi-objective low-fidelity optimization employed in the developed multi-fidelity methodology [17]. Also, EASY has demonstrated its success to handle a multi-objective Francis runner optimization problem [14].

3.3.1 NOMAD

Since NOMAD is a mesh adaptive method, it will stop when reaching the mesh convergence criterion even if the maximum number of evaluations is not used. NOMAD needs an initial design vector to start exploring the design space. Our previous investigations have indicated that in blade shape optimization problems, NOMAD performance and optimization results are quite sensitive to the initial design vector. In order to alleviate this drawback, a Latin Hypercube (LH) method has been used with 1% of the maximum computational budget, to evaluate 400 new design points at the beginning, and select the best one to obtain the most

promising initial vector.

Another important NOMAD aspect is the assignment of global search budget, which has been investigated in this study as well. Although the MADS algorithm is quite powerful in local search, it needs some special considerations to be successful in global search too. Variable Neighborhood Search (VNS) is an algorithm integrated into NOMAD to improve global search of the design space [25]. While the default value of VNS budget is equal to 75% of overall budget, two more global search budgets have been also investigated using VNS equal to 85% and 95% of the overall budget. The importance of global search is intensified in the problem at hand while the blade performance is strongly sensitive to small design variable changes.

All the constraints are considered as relaxable using the Progressive Barrier (PB) approach of NOMAD. With this approach, the MADS algorithm identifies new incumbent solutions by considering feasible points with the lowest objective values that improve feasibility. Optimization improvement is determined based on filter method of Fletcher and Leyffer [26].

3.3.2 EASY

A considerable number of evolutionary algorithm parameters have to be taken in to consideration in EASY. However, most of them have well-tuned default values. Based on previous investigations, the length of chromosomes (strings of binary digits representing values of design variables) and the population size (number of offspring generated in each iteration of evolutionary algorithm) have been chosen to be studied. Mutation- and cross recombination probabilities have been set to 0.02 and 0.9 respectively. Before each new geometry evaluation, EASY checks the database containing previous evaluated geometries to prevent repeating the same evaluation.

The evolutionary algorithms employed in EASY uses penalty functions to enforce constraints. For the problem at hand, proper constraint weights have been investigated and determined based on the ranges of infeasible constraints- and objective values.

4. Results and Discussions

For the problem at hand with the selected bounds of design variables, the lowest possible objective value is 1. Table 2 shows the results of the optimization problem defined in the last section using NOMAD and EASY. Feasible solutions are selected in the first step of the filtering process. As it was expected, EASY has achieved much larger numbers of feasible solutions due to its exceptional global search capacity. However, generally NOMAD is more capable in local search since it almost always has obtained the best possible objective value faster.

Table 2 NOMAD- and EASY-based optimization performances

			No. of Eval.	*No. of feasible solutions*	*First feasible solution*	*Obj. value of the first feasible*	*Best Obj. value*
NOMAD	VNS 0.75	X0	25679	0	-	-	-
		LH	15945	1460 (9.2%)	7981	1.04	1.00
	VNS 0.85	X0	37754	4175 (11.1%)	27191	1.14	1.00
		LH	27699	2494 (9.0%)	19039	1.07	1.00
	VNS 0.95	X0	40,000	1163 (2.9%)	5063	1.43	1.28
		LH	40,000	1412 (3.5%)	9176	1.09	1.00
EASY	P 50	L 5	40,000	25558 (63.9%)	1839	1.23	1.01
		L 10	40,000	25789 (64.4%)	1512	1.22	1.00
		L 15	40,000	10997 (27.5%)	2007	1.20	1.10
		L 20	40,000	23698 (59.2%)	1587	1.22	1.00
	P 30	L 10	40,000	0	-	-	-
	P 40	L 10	40,000	0	-	-	-
	P 60	L 10	40,000	15246 (38.1%)	8984	1.25	1.20
	P 70	L 10	40,000	0	-	-	-

Six NOMAD optimization results indicate LH search at the beginning of the optimization is really helpful, especially in lower VNS budgets. For instance, while using an initial design vector (i.e. X0) has led to no feasible solution, using LH to find a relatively good initial vector has improved extensively the performance and allowed achieving 1460 feasible solutions in 38% fewer number of evaluations (due to NOMAD mesh convergence stopping criterion). In this optimization the objective value of the first feasible solution was quite good which caused reaching the best possible objective value very quickly. The aforementioned point has been well demonstrated in Fig. 5. The bigger the VNS budget assigned, the more chance of globally exploring the design space and getting away from the local minima in order to find other good solutions. Disconnected curves in Fig. 5 (e.g. dedicated as VNS 0.95_LH) indicates that point, since each of those disconnections shows the VNS effect by stopping local search and jumping out of the previous search regions, which usually causes starting from new infeasible regions. This figure also indicates that NOMAD is really sensitive to the initial design vector and confirms the necessity of LH usage. For instance, using the highest VNS budget (i.e. 0.95) without LH, could not improve the relatively big objective value of the first feasible solutions. Although in this optimization the first feasible solution was obtained quite fast (at the 5063rd evaluation), completing all 40,000 evaluations did not lead to a better objective value than 1.28. Among NOMAD optimizations, VNS

0.85_LH has been chosen for further investigation since it has explored the design space with a medium global search budget with a relatively low number of evaluations due to quick local search convergence.

EASY optimization results indicate that it is really sensitive to the studied parameters, especially to the size of population. Thus, it should be carefully calibrated at the beginning. The best possible objective value has been achieved only by using the population of 50. No feasible solution has been obtained using population sizes of 30, 40 and 70. The results also indicate that among different chromosome lengths, lengths of 10 and 20 have resulted in the best objective value. A larger number of feasible solutions and a better convergence are achieved using length of 10 (see Fig 6). Therefore, it was selected for the investigation of population size effect. Also, the case with population size of 50 and length of 10 (called P50_ L10) has been chosen for further investigation.

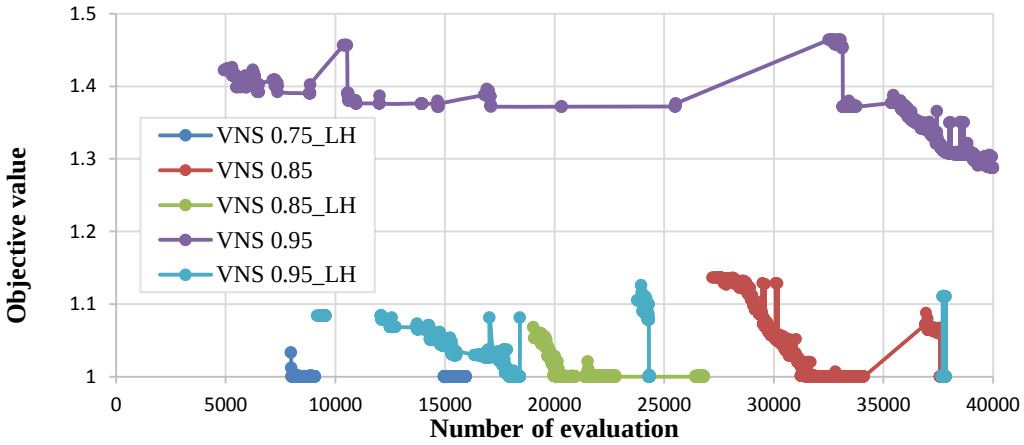

Fig. 5 Objective value improvement of feasible solutions obtained by NOMAD using different VNS budgets

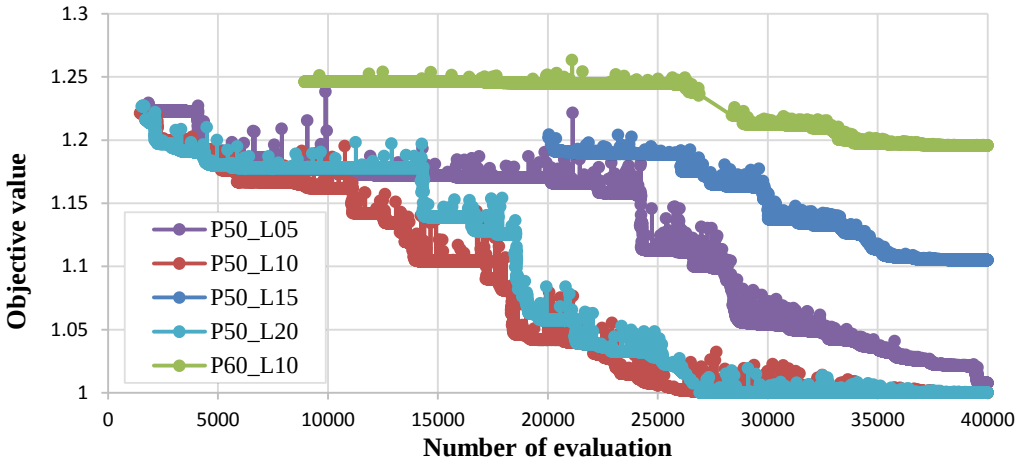

Fig. 6 Objective value improvement of feasible solutions obtained by EASY using different population sizes and chromosomes lengths

Global search capability of EASY can be illustrated by investigating the distribution of feasible solutions in the design space. For instance, Fig. 7 shows that distribution for two selected optimization results of NOMAD (VNS 0.85_LH) and EASY (P50_L10) from six design variable points of view. In all of them, EASY has covered significantly larger feasible regions. It is really important from the filtering point of view, since the main task of the filtering unit (see Fig. 2) is selecting a certain number of promising candidates while they are geometrically as different as possible. Figure 7 indicates that among the presented design variables, there is a big concentration of feasible solutions on the lower bounds of length design variables; thus, optimization improvement may be reached by decreasing those lower bounds. It was expected in advance since the objective function has been formulated as a summation of weighted length variables. However, as it was mentioned earlier, the lower bounds of length variables has been defined by experienced designers due to other design considerations, and consequently cannot be changed.

Figure 8 illustrates comparison of two selected optimization results with filtered candidates. As a good local optimizer, NOMAD converges quickly down to the best objective value once it achieves the first feasible solutions, although this achievement happens relatively late. However, EASY as a good global optimizer obtains a much larger number of feasible solutions from very earlier evaluations, but it improves the objective value gradually within some major recognizable steps.

Four promising candidates were chosen by the filtering unit for each of those two optimizations to be sent to high-fidelity phase. Table 3 shows the results of High-fidelity Navier-Stokes analyses of the selected candidates. It indicates that the 21988th solution of NOMAD optimization is the best selected candidate, which has the improved efficiency curve peak at the targeted power coefficient within the allowed error range (±1% error for the problem at hand), while it has no cavitating area. If none of those candidates has the peak position within the range, the candidate with the best efficiency (e.g. 22705) may be chosen to be

used as the new initial geometry for the next optimization step with corrected operating conditions. However, different selection policies may be applied for different situations.

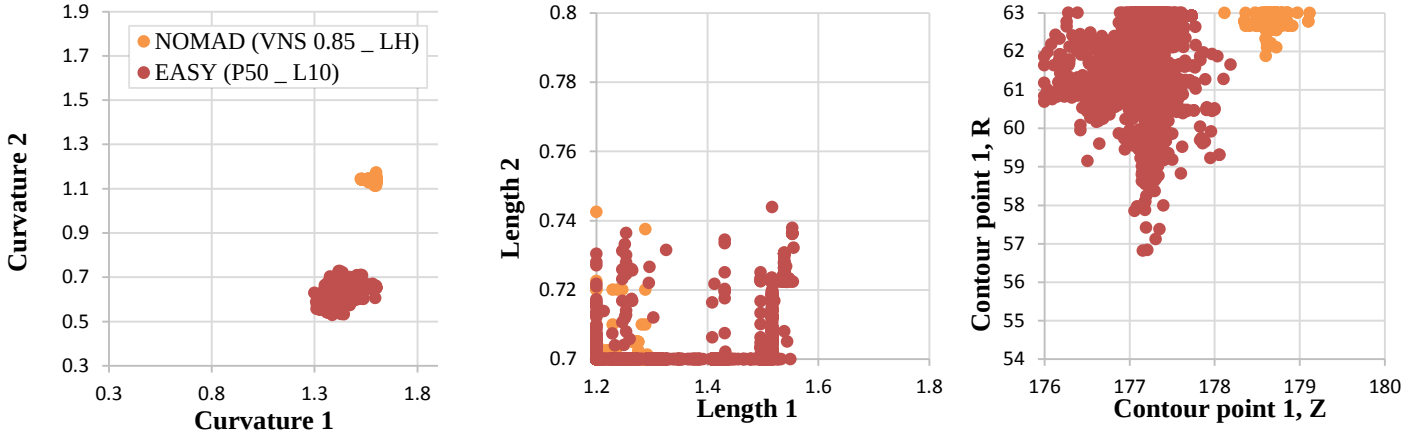

Fig. 7 Comparison of feasible solution distributions in the design space.

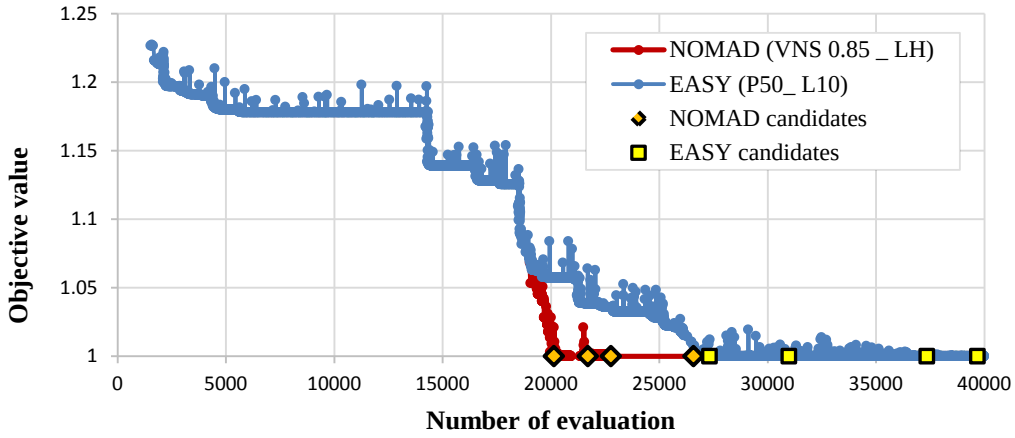

Fig. 8 Objective value improvement of feasible solutions obtained by the best NOMAD- and EASY optimizations

Table 3 High-fidelity evaluation results of filtered candidates

	Evaluation number	*Efficiency improvement (%)*	*Peak position deviation (%)*	*Cavitation existence*
NOMAD	20139	2.5	-1.6	No
	21988	2.4	-0.7	No
	22705	3.3	-2.1	No
	26587	1.8	0.1	Yes
EASY	27001	2.4	-1.5	No
	30989	2.1	-1.8	No
	37356	1.9	-0.9	Yes
	39686	2.3	-1.0	No

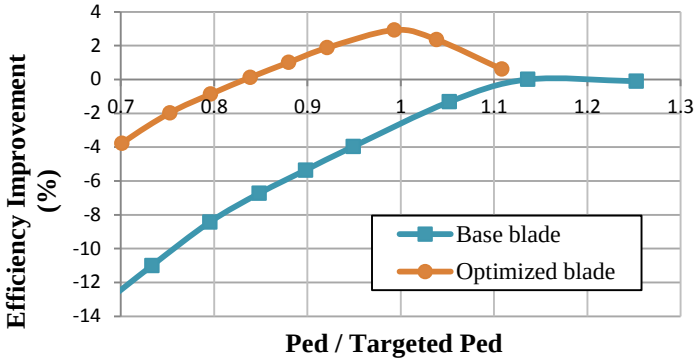

Fig. 9 Efficiency improvement of the optimized blade versus normalized power coefficient

The optimized blade is much shorter with a complex pattern of blade curvature. According to Fig. 9, using length objective with three well-defined constraints has led to considerable efficiency enhancement (2.4%) at the right operating condition. In this figure, efficiency improvement has been calculated from the peak efficiency of the base geometry. Comparison of Fig. 10 and 11 shows the improvement of low-fidelity pressure curves along the blade to satisfy the pressure constraint on the targeted operating condition. Pressure coefficients have been normalized with the minimum and the maximum coefficients of the optimized blade. These pressure curves are relatively consistent with high-fidelity results. The proper arrangement of pressure curves along the optimized blade sections has led to an appropriate blade loading and negative load prevention. Satisfaction of tangential velocity constraint has significantly improved the tangential velocity profile at the runner outlet on the targeted operating condition, which plays an important role to minimize energy losses and to maximize the efficiency (see Fig. 12).

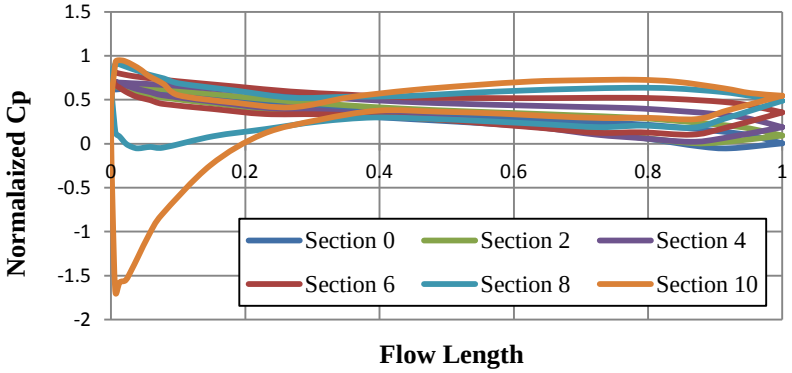

Fig. 10 Normalized pressure coefficient along the initial blade sections

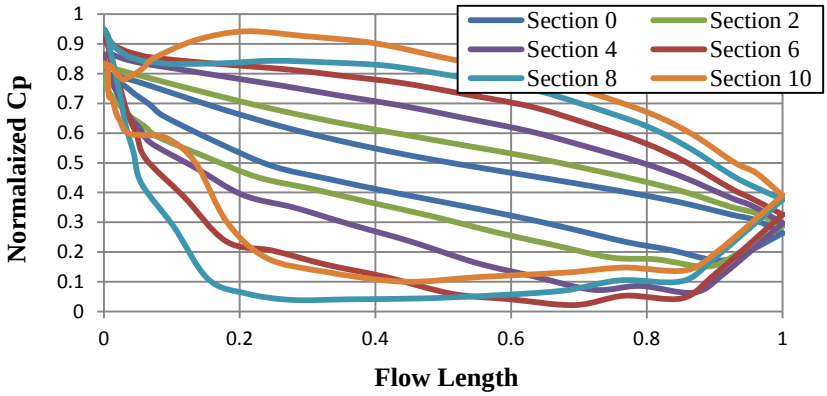

Fig. 11 Normalized pressure coefficient along the optimized blade sections

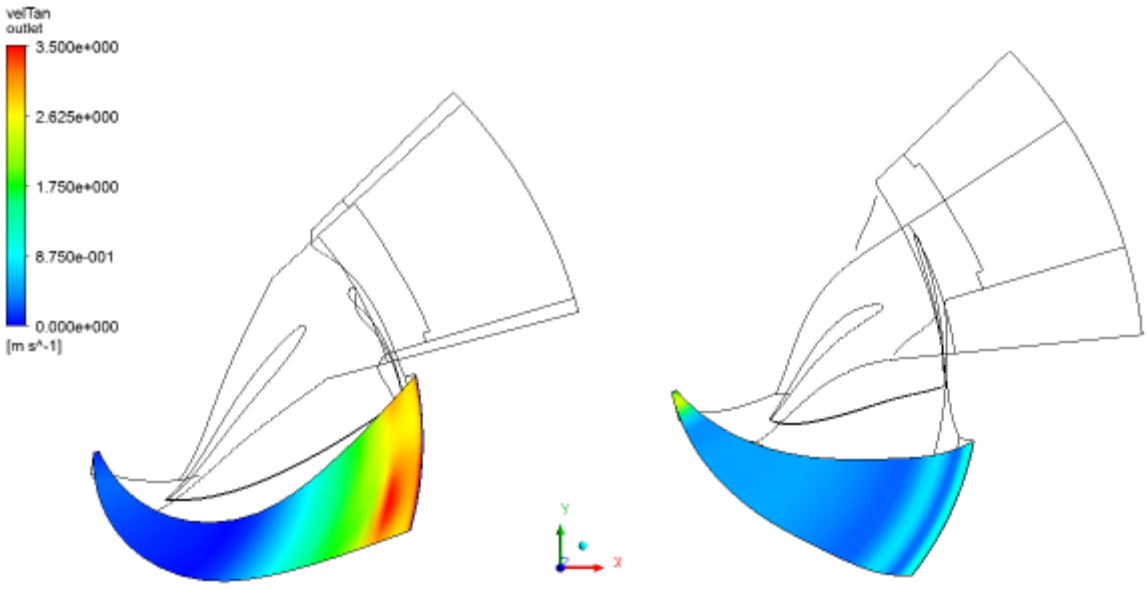

Fig. 12 Tangential velocity improvement at the runner outlet; left: base geometry, right: optimized geometry

The results indicate that no more design step is needed, since:

- All defined constraints have been satisfied in the first step.
- No relaxed constraint has been used in the optimization; so there is no need to increase the number of design variables to achieve feasibility of real constraints.
- High-fidelity evaluations have indicated that the main optimization target (i.e. right peak position) has been achieved properly, with a good efficiency. Therefore, no target correction is needed.

However, if there was a significant deviation from the targeted peak position, the operating condition used in the low-fidelity optimization constraints should be corrected in the next optimization step. We applied two linear corrections previously in optimizing a medium high-head Francis runner within three optimization overall loops [17]. Also, off-design operating points can be considered by adding new constraints and/or objectives dedicated to those operating conditions such as [21].

The optimized blade may be employed by designers as a good starting point to do very fine tunings in order to obtain other characteristics of a desired design. This final design step cannot be carried out within the optimization mainly due to the necessity of using a lot of geometrical parameters.

5. Conclusion

A robust multi-fidelity design optimization methodology has been developed to integrate advantages of high- and low-fidelity analyses, aiming to help designers to reach efficient turbine runners in reasonable computational time and cost. In the low-fidelity phase the automatic optimization loop is in charge of providing a lot of solutions using fast low-fidelity inviscid flow evaluations as a physic-based surrogate model. Considering important challenges of the design environment (such as non-linear non-convex design spaces), NOMAD and EASY have been chosen. NOMAD uses the MADS algorithm, which has demonstrated its power of local search in complex industrial applications. EASY employs an evolutionary algorithm, which is quite well-known for its global search capability.

Since the low-fidelity solver used in the optimization is not accurate enough and the efficiency is not directly reachable, a filtering unit selects a limited number of geometrically different candidates which are dominant in their own neighborhoods. The computationally expensive high-fidelity phase is responsible for evaluating those candidates and choosing the best. These accurate results are valuable as well to calibrate low-fidelity optimization by the optimization correction unit.

The developed methodology demonstrated its advantages by designing a low-head Francis runner through a relatively low computational cost. Although the initial geometry was quite poor, all design targets were met in the first optimization step without any optimization tuning. The design targets were relatively simplified and only associated to the peak operating point. In the case of using more complicated targets with more design points, it is expected to use more optimization steps, corrected by high-fidelity results.

NOMAD and EASY optimization results indicate that each of them has its own abilities and drawbacks for the problem at hand, which come from the algorithms each of the optimizers employ. It may be concluded that for such a complex optimization problem, combining those two optimization algorithms can bring more optimization efficiency, while alleviates their disadvantages. While NOMAD, even assisted with LH, could not obtain the feasibility up to around 10,000 evaluations (25% of the maximum evaluation budget), EASY always achieves very big percentages of feasible solutions, without difficulty from about 1000 evaluations to the end of optimization. Therefore, it is a good candidate to apply for the first round of low-fidelity optimization, in order to have a wide global search of the design space within a couple of thousands evaluations. In the second round, NOMAD will gain from those promising feasible solutions obtained by EASY for deep local searches. NOMAD has proved its high performance to do the aforementioned task within a very few evaluations. By applying this new methodology, it is

possible to cut significant computational cost and time, and achieve better optimized blade as a result of a better design space exploration.

Acknowledgments

The authors would like to thank Andritz Hydro Canada Inc. and NSERC, Natural Sciences and Engineering Research Council of Canada, for supporting this project. They also would like to gratefully acknowledge Nigel Murry, Christophe Devals, Maxime Gauthier and Evgenia Kontoleontos at Andritz Hydro Canada Inc. and Andritz Hydro GmbH for their contributions.

References

[1] G. Holmes and J. Y. McNabb, "Application of three-dimensional finite element potential flow analysis to hydraulic turbines," presented at the International Symposium on Refined Modeling of Flows, Paris, France, 1982.

[2] J. M. Franco-Nava, E. R. Tamariz, O. D. Gomez, J. M. F-Davila, and R. R-Espinosa, "CFD performance evaluation and runner blades design optimization in a Francis turbine," ASME 2009 Fluids Engineering Division Summer Meeting, Colorado, USA, 2009.

[3] I. M. Pilev, A. A. Sotnikov, V. E. Rigin, A. V. Semenova, S. G. Cherny, D. V. Chirkov, *et al.*, "Multiobjective optimal design of runner blade using efficiency and draft tube pulsation criteria," *IOP Conference Series: Earth and Environmental Science*, vol. 15, 032003, 2012.

[4] S. Derakhshan and N. Kasaeian, "Optimal design of axial hydro turbine for micro hydropower plants," *IOP Conference Series: Earth and Environmental Science*, vol. 15, 042029, 2012.

[5] H. Georgopoulou, S. Kyriacou, K. Giannakoglou, P. Grafenberger, and E. Parkinson, "Constrained Multi-Objective Design Optimization of Hydraulic Components Using a Hierarchical Metamodel Assisted Evolutionary Algorithm. Part 1: Theory'," *24th IAHR Symposium on Hydraulic Machinery and Systems, Foz do Iguassu, Brazil*, 2008.

[6] N. M. Alexandrov, R. M. Lewis, C. R. Gumbert, L. L. Green, and P. A. Newman, "Optimization With Variable-Fidelity Models Applied to Wing Design," NASA Langley Technical Report Server, 2000.

[7] T. D. Robinson, M. S. Eldred, K. E. Willcox, and R. Haimes, "Surrogate-Based Optimization Using Multifidelity Models with Variable Parameterization and Corrected Space Mapping," *AIAA Journal*, vol. 46, pp. 2814-2822, 2008.

[8] L. Leifsson and S. Koziel, "Variable-Fidelity Aerodynamic Shape Optimization," in *Computational Optimization, Methods and Algorithms*. vol. 356, S. Koziel and X.-S. Yang, Eds., ed: Springer Berlin Heidelberg, pp. 179-210, 2011.

[9] S. Bahrami, C. Tribes, S. von Fellenberg, T. C. Vu, and F. Guibault, "Multi-fidelity design optimization of Francis turbine runner blades," *IOP Conf. Ser.: Earth Environ. Sci.*, vol. 22, 012029, 2014.

[10] S. Le Digabel, "Algorithm 909: NOMAD: nonlinear optimization with the MADS algorithm," *ACM Transactions on Mathematical Software*, vol. 37, pp. 44-59, 2011.

[11] M. Abramson, C. Audet, G. Couture, J. Dennis, S. L. Digabel, and C. Tribes. *The NOMAD project*. Available: http://www.gerad.ca/nomad

[12] M. A. Abramson, C. Audet, J. E. Dennis, Jr., and S. Le Digabel, "ORTHOMADS: a deterministic MADS instance with orthogonal directions," *SIAM Journal on Optimization*, vol. 20, pp. 948-966, 2009.

[13] K. C. Giannakoglou. (2008). *The EASY (Evolutionary Algorithms SYstem) software*. Available: http://velos0.ltt.mech.ntua.gr/EASY

[14] S. Kyriacou, E. Kontoleontos, S. Weissenberger, L. Mangani, E. Casartelli, I. Skouteropoulou, *et al.*, "Evolutionary algorithm based optimization of hydraulic machines utilizing a state-of-the-art block coupled CFD solver and parametric geometry and mesh generation tools," *IOP Conf. Ser.: Earth Environ. Sci.*, vol. 22, 012024, 2014.

[15] J. McNabb, C. Devals, S. A. Kyriacou, N. Murry, and B. F. Mullins, "CFD based draft tube hydraulic design optimization," *IOP Conf. Ser.: Earth Environ. Sci.*, vol. 22, 012023, 2014.

[16] S. A. Kyriacou, "Evolutionary Algorithm-based Design-Optimization Methods in Turbomachinery," PhD PhD thesis, National Technical University of Athens, 2013.

[17] S. Bahrami, C. Tribes, C. Devals, T. C. Vu, and F. Guibault, "Multi-objective optimization of runner blades using a multi-fidelity algorithm," in *ASME 2013 Power Conference*, Boston, USA, 2013.

[18] M. Gauthier, "StageX Package," Andritz Hydro Canada Inc., 2012.

[19] T. C. Vu, C. Devals, Z. Ying, B. Nennemann, and F. Guibault, "Steady and unsteady flow computation in an elbow draft tube with experimental validation," *International Journal of Fluid Machinery and Systems*, vol. 4, pp. 84-95, 2010.

[20] T. C. Vu, M. Gauthier, B. Nennemann, M. Koller, and C. Deschenes, "Flow simulation for a propeller turbine with different runner blade geometries," in *26th IAHR Symposium on Hydraulic Machinery and Systems, August 19, 2012 - August 23, 2012*, Beijing, China, 2012.

[21] S. Bahrami, C. Tribes, C. Devals, T. C. Vu, and F. Guibault, "Multi-fidelity shape optimization of hydraulic turbine runner blades using a multi-objective mesh adaptive direct search algorithm," *Applied mathematical modelling*, accepted.

[22] R. Susan-Resiga, S. Muntean, P. Stein, and F. Avellan, "Axisymmetric Swirling Flow Simulation of the Draft Tube Vortex in Francis Turbines at Partial Discharge," presented at the 24th Symposium on Hydraulic Machinery and Systems, Brazil, 2009.

[23] S. Tridon, S. Barre, G. D. Ciocan, and L. Tomas, "Experimental analysis of the swirling flow in a Francis turbine draft tube: Focus on radial velocity component determination," *European Journal of Mechanics, B/Fluids*, vol. 29, pp. 321-335, 2010.

[24] N. Murry, "Xmt Overview," Andritz Hydro Canada Inc., 2010.

[25] C. Audet, V. Béchard, and S. Digabel, "Nonsmooth optimization through Mesh Adaptive Direct Search and Variable

Neighborhood Search," *Journal of Global Optimization,* vol. 41, pp. 299-318, 2008.
[26] R. Fletcher and S. Leyffer, "Nonlinear programming without a penalty function," *Mathematical Programming,* vol. 91, pp. 239-269, 2002.